CrossMark

Visible-Light-Driven Photocatalytic N-Doped TiO$_2$ for Degradation of Bisphenol A (BPA) and Reactive Black 5 (RB5) Dye

Roziana Kamaludin · Mohd Hafiz Dzarfan Othman · **Siti Hamimah Sheikh Abdul Kadir · Ahmad Fauzi Ismail · Mukhlis A. Rahman · Juhana Jaafar**

Abstract Bisphenol A (BPA) and reactive black 5 (RB5) dye are among the most persistent and non-biodegradable contaminants in water which require an urgent need for the development of effective removal method. The ubiquitous existence of both contaminants could interfere with the human health and aquatic environmental balance. Photocatalytic process as one of advanced oxidation processes (AOPs) has shown high performance for degradation of organic compounds to the harmless materials under sensible condition. Therefore, this study aims to develop a visible-light-driven photocatalyst that can efficiently degrade BPA and RB5 present in household water. N-doped TiO$_2$ were successfully synthesized via simple and direct sol–gel method. The prepared TiO$_2$ nanoparticles were characterized by field emission scanning microscope (FE-SEM), X-ray diffraction (XRD), Fourier transform infrared (FTIR), and Brunauere Emmette Teller (BET) analysis. The incorporation of nitrogen in TiO$_2$ lattice exhibited excellent optical responses to visible region as revealed by UV–Vis–NIR spectroscopy absorption capability at 400–600 nm. The photocatalytic activity of the N-doped TiO$_2$ nanoparticles was measured by photocatalytic degradation of BPA and RB5 in an aqueous solution under visible-light irradiations. Degradation of BPA and RB5 was 91.3% and 89.1%, respectively after 360 min illumination. The degradation of BPA and RB5 by N-doped TiO$_2$ was increased up to 89.8% and 88.4%, respectively under visible-light irradiation as compared to commercial TiO$_2$ P25. This finding clearly shows that N-doped TiO$_2$ exhibits excellent photocatalytic degradation of BPA and RB5 under visible irradiation, hence have a promising potential in removing various recalcitrant contaminants for water treatment to fulfill the public need to consume clean water.

Keywords N-doped TiO$_2$ · Bisphenol A · RB5 · Photocatalysis · Visible light active · Sol–gel method

R. Kamaludin · M. H. D. Othman (✉) · A. F. Ismail · M. A. Rahman · J. Jaafar
Advanced Membrane Technology Research Centre (AMTEC), School of Chemical and Energy Engineering, Universiti Teknologi Malaysia (UTM), 81310Skudai, Johor Bahru, Johor, Malaysia
e-mail: hafiz@petroleum.utm.my

S. H. S. A. Kadir
Institute of Medical Molecular Biotechnology, Faculty of Medicine, Sungai Buloh Campus, Universiti Teknologi MARA (UiTM), Jalan Hospital, 47000 Sungai Buloh, Selangor, Malaysia

1 Introduction

Globally, numerous contaminants have been identified in various source of water such as bisphenol A (BPA) and reactive black 5 (RB5) dye which has been linked with many adverse health effects towards human and aquatic animals. BPA 2,2-bis(4-hydroxyphenyl)propane, with two unsaturated phenol rings (Vandenberg et al. 2007), is the most studied endocrine disruptor compounds (EDCs) and one of the major contaminants of household water. Meanwhile, RB5 with two N=N groups which known as "azo"

Springer

groups (Zainudin et al. 2016) constitute over 50% of all textile dyes (Tang and An 1995), hence it is one of major textile industrial polluter. BPA is an organic compound, highly produced synthetic monomer (Vandenberg et al. 2007) which is employed in the in the manufacture of polycarbonate (PC) plastics, epoxy resins (Lenie et al. 2008; Grasselli et al. 2010), and as a stabilizer in polyvinyl chloride (PVC) (Li et al. 2010). BPA is also used in food and drinks polycarbonate plastic packaging, sports equipment, plastic toys, dental sealants, and composite (Vandenberg et al. 2007; Lenie et al. 2008) and therefore, it is considered that leaching from such materials is one of the contamination sources of BPA in the surface water and environment. Since decades ago, the presence of BPA in household water has become major concerns among public because the widespread existence of BPA in household water, drinking water, surface water, and the surrounding environment results in a preventable exposure to human and animals. To make it worse, prolonged exposure to the contaminated level of BPA could interfere with human body system such as hormones regulation and cell signaling pathways. Human exposure to BPA has been linked with various health threats including increase carcinogenic and cardiovascular risk (Li et al. 2010), decrease sperm production and quality (Milić et al. 2015), influence on preimplantation development (Takai et al. 2000), thyroid function disruption (Meeker and Ferguson 2011), obesity (Takeuchi et al. 2004), and diabetes (Lang 2008). In the meantime, reactive black 5 (RB5) is one of the most popular reactive dye with two N=N groups which known as "azo" groups (Zainudin et al. 2016). RB5 become more attractive option in the textile industries because it show great feature such as bright and high-intensity colors as well as they have quite good fastness properties. Importantly, RB5 relatively can be purchase at low cost in addition to the simplicity of the reactions which process can be scaled up or down very easily. However, wastewater from the effluent of textile industries are often rich in color, containing residues of reactive dyes and chemicals, such as complex components, many aerosols, high chroma, high-chemical oxygen demand (COD), and biochemical oxygen demand (BOD) concentration as well as much more hard-degradation materials (Balakrishnan et al. 2008). The resistance of RB5 to detergents will allow the dyes to convert into more stable, non-biodegradable, and toxic molecules even at a low concentration. Therefore, small amounts of dye are clearly visible, detrimental to the water environment (Shah and Patel 2014), and toxic to its creatures (Lazim et al. 2015). Furthermore, the ecological

balance of aquatic system was affected by the accumulation of dyes in sediments at sites of landfill and wastewater discharge. Additionally, the human exposure to the dyes can cause allergic dermatitis and skin irrigational (Ugurlu et al. 2007). Clearly, all those threats have led to the increasing public demand of clean water sources which excites a challenge for the contaminants removal processes.

Both structures of BPA and RB5 are made up of strong bonds thus both contaminants are not easily biodegradable, metabolized, or broken down into less toxic compound compared to other contaminants. Hence, at the moment, the conventional treatment processes such membrane filtration, adsorption, and bioreactor-based membrane and bioreactors are not able to completely remove both contaminants. These lead to the emerging of advanced process for rapid contaminants degradation in contaminated sources are highly required. Advanced oxidation processes (AOPs) of photocatalysis has shown high performance for degradation of organic compounds to the harmless materials under sensible condition due to several advantages include complete mineralization and up to 90% degradation efficiency in treating organic compounds at low concentrations (O'Shea and Dionysiou 2012) in addition to oxidizing organic compound into nontoxic substances, such as CO_2 and H_2O (Umar and Abdul Aziz 2013).

Titanium dioxide (TiO_2) is widely used semiconductors photocatalyst in water and wastewater treatment (Liu et al. 2015). TiO_2 is often chosen as a photocatalyst due to its superhydrophilicity (Wang et al. 1997), strong oxidizing abilities for degradation of organic compounds (Jańczyk et al. 2006), and long-term chemical stability (Lee et al. 2011), in addition to inexpensive and nontoxicity properties (Nakata and Fujishima 2012). Although photocatalysis is efficient, the band gap of the pure TiO_2 particles is a major bottleneck that limits the application of these photocatalytic processes for treating the contaminants (Mohamed et al. 2015a). The width of band gap is one of the most important properties which strongly influence the electrical and optical properties of the material. Broader band gap needs more energy to excite the electrons which means only the irradiation carrying higher energy such as ultraviolet light and microwave can be used for the energy source during the reaction process. The irradiation with lower energy, visible light, and infrared, for example, can only drive catalysts with narrow band gap (Chen et al. 2016).

Pure TiO$_2$ particles have large band gap up to 3.2 eV; therefore pure, TiO$_2$ particles only displays its photocatalytic properties under ultraviolet light ($\lambda \leq 387$ nm), thus limiting the photocatalyst efficiency for visible-light applications (Pelaez et al. 2012). The higher end of UV spectrum usually required high operating costs (Chong et al. 2010) which become other main disadvantages in the production of large-scale industrial photochemical synthesis. Therefore, it is important to improve the photocatalytic activity of TiO$_2$ for visible-region applications. In contrast, pure TiO$_2$ particles alone cannot function effectively when irradiated with visible light, such as fluorescent light, which contains a very small amount of UV light.

Recently, there is emerging interest in developing method to increase the sensitivity of TiO$_2$ to visible light via non-metal elemental doping due to their efficiency to lower the band gap. Among non-metal dopants, nitrogen has been observed as one of the promising materials for TiO$_2$ lattice to induce visible absorption (Lee et al. 2014) mainly because of its comparable atomic size with oxygen (Viswanathan and Krishanmurthy 2012). Besides, nitrogen exhibits small ionization energy, eco-friendly, higher stability, and simple synthesis methods (Gai et al. 2012; Zhang et al. 2013) for an ideal dopant material. The introduction of nitrogen into TiO$_2$ lattice structure is believed to narrow the band gap of TiO$_2$, thus provide efficient photocatalytic activity under visible-light irradiation (Ruzimuradov et al. 2014). The incorporation of nitrogen into TiO$_2$ either in the bulk or as a surface dopant has been explored via both dry and wet preparation methods (Pelaez et al. 2012). Sputtering deposition (Abadias et al. 2010) and ion implantation (Jinlong et al. 2010) rely on the direct treatment of TiO$_2$ with energetic nitrogen ions. Meanwhile, various other methods have been successfully applied to prepare N–TiO$_2$ such as gas-phase reaction methods (Kafizas et al. 2010), atomic layer deposition (Zhao et al. 2008), and pulsed laser deposition (Pore et al. 2006). However, the sol–gel method is the most versatile and easy technique for the synthesis of N-doped TiO$_2$ nanoparticles is due to its simple equipment and permits fine control of the material's nanostructure and morphology. To date, there is hardly a report on the preparation of nitrogen doped to degrade BPA and RB5. Therefore, this study aims to develop a visible-light-driven N-doped TiO$_2$ photocatalyst for the efficient degradation of BPA and RB5 present in water. Thus, in this study, N-doped TiO$_2$ with broad range UV and visible light absorbing capacity was prepared via simple sol–gel method. The morphological properties, crystallinity, and optical properties of the prepared N-doped TiO$_2$ had been characterized using SEM, FE-SEM, EDX, XRD, BET, FTIR, and UV–VIS–NIR. Finally, the photocatalytic activity of the prepared N-doped TiO$_2$ nanoparticles was evaluated by using suspension photocatalytic reactor. N-doped TiO$_2$ nanoparticles were used as it is and its efficiency was evaluated by photodegradation of BPA and RB5 in aqueous solution under visible-light irradiation and comparison study under UV light as well. Interestingly, the degradation of BPA and RB5 would be a great chance to provide an early insight on the potential role of visible-light-driven photocatalytic N-doped TiO$_2$ for complete degradation and removing of colored and non-colored recalcitrant in wastewater as well as to remove their adverse health effects.

2 Experimental

2.1 Materials

Titanium-n-butoxide (Ti(OBu$_4$)) purchased from Sigma-Aldrich was used as a titanium precursor. Nitric acid (HNO$_3$) 65% and isopropanol (C$_3$H$_7$OH) were obtained from QReC Chemicals. HNO$_3$ was used as the catalyst and also as the nitrogen source; meanwhile, isopropanol and distilled water were used as the dispersing media. Commercial TiO$_2$ Degussa P25 (TiO$_2$ P25) purchased from Sigma-Aldrich was used in the control experiment. BPA and RB5 are supplied by Sigma-Aldrich (USA) was analytical reagent grade and was used as received, without further purification. All chemicals used were of analytical reagent grade and were used as received without further dilution.

2.2 Photocatalyst Preparation

A sol–gel method adapted from previous study (Mohamed et al. 2015a) was applied to synthesize N-doped TiO$_2$. As shown in Fig. 1, 25 mL of Ti(OBu)$_4$ was dissolved in 8 mL of isopropanol under constant magnetic stirring at 50 °C. The homogeneous mixture was subsequently added dropwise into 200 mL of distilled water under vigorous stirring for 30 min, followed by the addition of 3 mL of HNO$_3$ 65% dropwise into the mixture under vigorous stirring for about 60 min. Then, the homogeneous sol was aged in air-tight container at
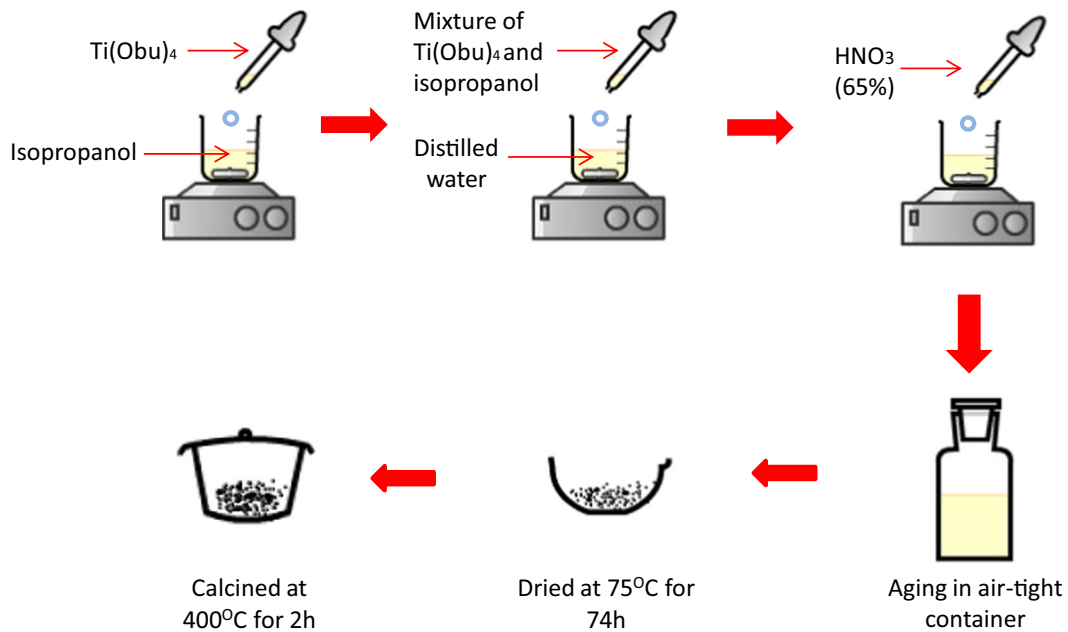
Fig. 1 Sol–gel method of the N-doped TiO$_2$ preparation

room temperature for 3 days until the formation of yellowish gel. The resultant yellowish gel then was dried at 70 °C for 72 h to obtain a yellowish solid powder. The obtained yellowish powder was ground and subjected to calcination at 400 °C for 2 h. Calcination treatment was carried out in the furnace at 5 °C min^{-1}. The resultant powder then was washed with distilled water several times and finally washed with isopropanol. Subsequently, the powder was further dried at 60 °C for 24 h. The prepared N-doped TiO$_2$ was stored in covered container until further used.

2.3 Characterization

2.3.1 Morphological Properties Analysis

The morphological nature of prepared N-doped TiO$_2$ was explored qualitatively by scanning electron microscopy (SEM; Model: TM 3000, Hitachi) and field emission scanning electron microscopy (FE-SEM; Model: SU2080, Hitachi) at an accelerated voltage of 2.0 kV. The presence of nitrogen in the prepared TiO$_2$ sample was investigated using the line scan of spectrum of energy dispersion of X-ray (EDX; Model: X-MaxN 51-XMX1011, Oxford Instrument). The sample was positioned on a metal holder and then was sputter coated with gold under vacuum approximately for 3 min. The morphological study of the sample was examined at various magnifications and the presence of nitrogen was scan randomly by EDX.

2.3.2 X-Ray Diffraction (XRD) and Brunauer, Emmet, and Teller (BET) Analysis

The crystallinity and the phase formation of the prepared TiO$_2$ sample was analyzed using an X-ray diffractometer (XRD; Model: D5000, Siemens). The measurements were carried out at 40 kV and 40 mA, which employed a CuKα radiation at a wavelength of 0.15418 nm at an angular incidence of 2θ = 20–80° with a scan step speed of 1°/min. The surface areas were calculated by using the BET surface area measurement by nitrogen adsorption–desorption analysis. The prepared N-doped TiO$_2$ was degassed at 250 °C prior to BET measurement using a Micromeritics (3Flex, Version 3.01, USA). To calculate the weight fraction between anatase and rutile, the following equation (Ananpattarachai et al. 2009) was followed:

$$WR = \frac{Ar}{0.884Aa + Ar} \tag{1}$$

where Ar represents the integrated intensity of the rutile (110) peak, and Aa is the integrated intensity of the anatase (101) peak.

In the meantime, the average sizes of anatase and rutile crystallite were estimated using the Scherrer formula (Moharram et al. 2014):

$$D = \frac{K\lambda}{\beta\cos\theta} \qquad (2)$$

where the K constant is taken to be 0.94, λ is the wavelength of the CuKα radiation source, and β the full width at half maximum (FWHM-in radians) of the diffraction peak corresponding to the Bragg diffraction angle (2θ).

2.3.3 Fourier Transform Infrared Spectroscopy

The presence of N-dopant in the TiO$_2$ sample was investigated by Fourier transform infrared (FTIR) spectroscopy using Perkin Elmerr FTIR ATR spectrophotometer with diamond ATR sampling accessory. The prepared sample was in direct contact with ATR diamond by clamping the sample to the diamond surface and was scanned with the wave number ranging from 4000 to 650 cm^{-1}.

2.3.4 UV–Visible Spectroscopy

The UV–Vis spectra were used to examine the optical property of the prepared N-doped TiO$_2$ sample on the light absorption capability under UV and visible-light irradiation. For N-doped TiO$_2$ powder samples, KBr method has been employed for analysis. Sample was clamped to the sample holder and scanned between 200 and 600 nm using UV–Vis–NIR spectrophotometer (Model: UV-3101PC, Shidmadzu). From UV–Vis–NIR spectra, the band gap energy of the prepared N-doped TiO$_2$ sample was estimated using the following equation (Dharma and Pisal 2009):

$$\text{Band gap energy } (E) = \frac{(h \times C)}{\lambda} \qquad (3)$$

where h is planks constant, C is the speed of light, and λ is the cut of wavelength.

2.4 Photocatalytic Activity Measurement

In order to evaluate the photocatalytic activity of the prepared N-doped TiO$_2$, both BPA and RB5 solutions as synthetic contaminated household water were used as water pollutants. Prior to photocatalytic measurement, the adsorption capacity of the prepared N-doped TiO$_2$ nanoparticles was evaluated via adsorption test in aqueous solution. The photocatalyst was added into the pollutant solutions. The mixture was stirred continuously with a magnetic stirrer without any light irradiation. Ten-milligram suspensions were then collected at 10-min interval using 0.45 μm polyamide syringe filter to eliminate excess catalyst prior to analysis. The suspension of BPA and RB5 was subjected to high-performance liquid chromatography analysis (HPLC, Agilent Technologies 1260 Affinity) coupled with UV detector at 280 nm and Perkin Elmer UV–visible spectrophotometer at 597 nm, respectively. In the meantime, the photocatalytic degradation of BPA was evaluated under UV and visible-light irradiation. The photocatalyst was irradiated with visible light-emitting diode (LED Flood Light; Model: IP66, 30 W) and UV (Vilber Laurmat, k = 312 nm, 30 W) light. An air diffuser was used to provide sufficient oxygen (O$_2$) for the reaction. The prepared N-doped TiO$_2$ (0.5 g) was added in an aqueous solution containing 500 ml of BPA with a concentration of 6 ppm. The suspension was stirred in dark place for 30 min to reach adsorption–desorption equilibrium. The suspension (10 ml) was taken through 0.45 μm polyamide syringe filter to eliminate excess photocatalyst prior to analysis and treated as initial concentration (Co). Subsequently, the suspension was irradiated using white LED flood light/UV light and the suspension was collected as regular time interval (C_t), every 30 min for 6 h during irradiation and filtered through syringe filter. The same procedures were repeated for RB5 contaminant. The differential absorbance of irradiated BPA and RB5 samples with time throughout the experiment were measured by HPLC and UV–visible spectrophotometer, respectively. The photocatalytic activity was expressed in the percentage of BPA degradation according to the following equation:

$$\text{Degradation of BPA} = \frac{Co - Ct}{Ct} \times 100 \qquad (4)$$

where C_o is the initial concentration at time $t = 0$, and C_t is the concentration at time (t). Similar experiment was carried out for the commercial TiO$_2$ P25 under visible and UV-light irradiations for comparison study.

3 Results and Discussion

3.1 Morphological Characterization

The morphological nature of the prepared N-doped TiO$_2$ powder was investigated using SEM as shown in Fig. 2. The crystallize structure of N-doped TiO$_2$ powder was
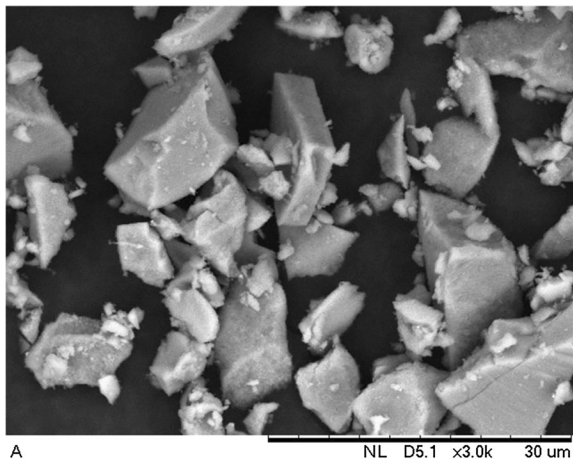
Fig. 2 SEM image of N-doped TiO$_2$ powder

Fig. 4 XRD pattern of N-doped TiO$_2$ sample

observed with estimated average length of below 160 μm and average width of 70 μm. The prepared N-doped TiO$_2$ powder was further characterized using FE-SEM microscopy analysis. The FE-SEM images of prepared sample as shown in Fig. 3 revealed that the formation of TiO$_2$ microspheres (Fig. 3b) is constituted by assembled TiO$_2$ nanorods (Fig. 3c) with estimated average length of below 60 nm and average width of 29 nm. Similar morphological findings were reported by previous studies (Mohamed et al. 2015b; Ruan et al. 2013). The formation of TiO$_2$ microspheres results was consistent with the XRD analysis (Section 3.2).

3.2 XRD and BET Analysis

XRD analysis is used to identify the presence of crystallite phase in the prepared TiO$_2$ sample. The XRD diffraction patterns of the prepared TiO$_2$ shown in the Fig. 4 demonstrated that diffraction peak of anatase (101) and rutile (110) was observed at $2\theta = 25.4°$ and $2\theta = 27.5°$. The percentages of rutile and anatase were
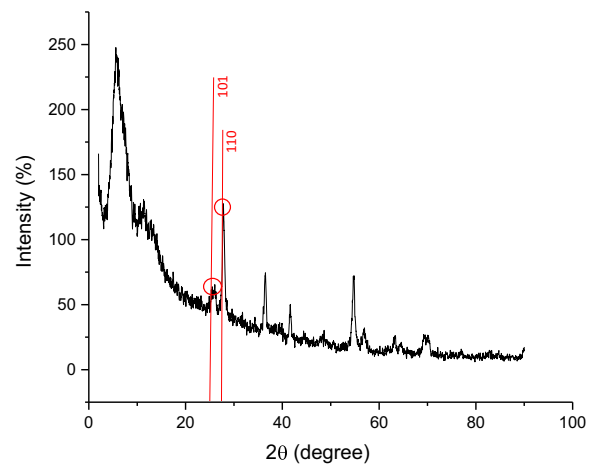
61% and 39%, respectively, thus suggested that the prepared TiO$_2$ is the anatase/rutile mixed phase TiO$_2$. The average sizes of anatase and rutile crystallite estimated using the Scherrer equation show that anatase and rutile crystallite were 14 and 26 nm respectively, and 20 nm in average. The specific surface area of the prepared N-doped TiO$_2$ determined by N$_2$ adsorption–desorption isotherms shows that the BET-specific surface area of the prepared N-doped TiO$_2$ is 49.64 m^2/g, which is slightly lower compared to commercial TiO$_2$ P25 (52 m^2/g) (Mohamed et al. 2015b). It is indicated that the prepared N-doped TiO$_2$ had slightly bigger crystallite size, which might promote comparable photocatalytic active surface sites per unit catalyst mass as compared to commercial TiO$_2$ P25.

3.3 FTIR Analysis and EDX Mapping

FTIR spectra were used to examined the presence of N-dopant in the prepared N-doped TiO$_2$ sample. Figure 5 shows the FTIR spectra of the synthesized
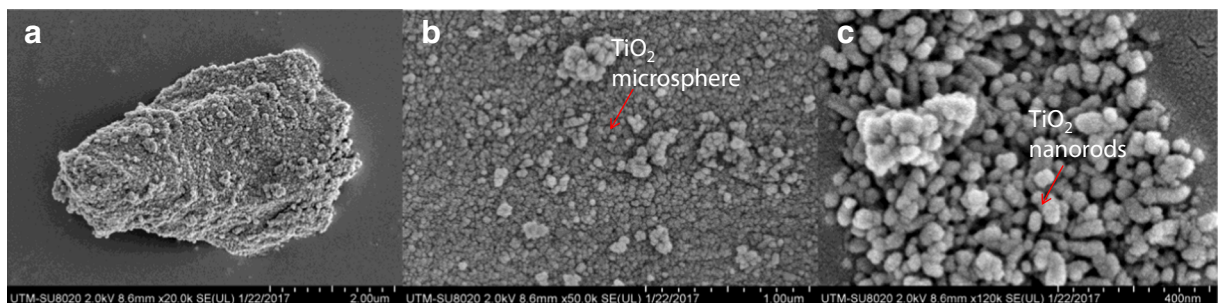

Fig. 3 FE-SEM images of N-doped TiO$_2$, **a** N-doped TiO$_2$ particle, **b** N-doped TiO$_2$ microsphere, and **c** N-doped TiO$_2$ nanorods
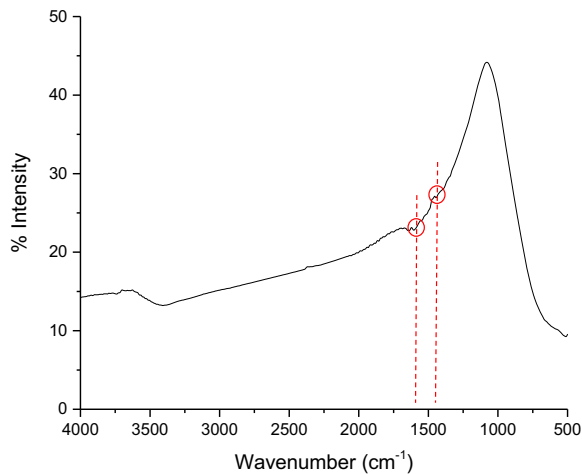
Fig. 5 FTIR pattern of N-doped TiO_2 sample

N-doped TiO_2 in the wave number range of 650–4000 cm^{-1}. As can be seen, the peaks around 1500–1600 and 1300–1390 cm^{-1} in samples N-doped TiO_2 are due to the presence of and NO_2^- species. The presence of these two peaks indicate that NO_2^- species could be chemisorbed on the surface of the synthesized N-doped TiO_2 and not affected as they had undergone calcination processes up to 400 °C. Similar finding can also be found in previously reported study (Mohamed et al. 2015a, b), where

they reported peaks around 1346 and 1095 cm^{-1} in their samples due to the presence of $N_2O_2^{2-}$ and NO^- species. The presence of the N-dopant was further confirmed with EDX mapping analysis (Fig. 6). As can be seen in Fig. 6, nitrogen and titanium species as N-dopant were detected in the prepared TiO_2 sample, hence nitrogen doping in TiO_2 lattice structure prepared via simple sol–gel method, indeed produce N-doped TiO_2. The introductions of nitrogen in the TiO_2 lattice structure are believed to increase the capability of the prepared TiO_2 to absorb higher fraction of photons from the visible region (Qiao et al. 2010; Hu et al. 2014) as evidence by UV–Vis–NIR spectroscopy analysis.

3.4 UV–Visible Spectroscopy

The optical response of the prepared N-doped TiO_2 was investigated by means of UV–Vis absorption spectra, as shown in Fig. 6. The prepared N-doped TiO_2 exhibited excellent visible region, thus the uses of HNO_3 as nitrogen doping sources are significantly improved the absorbance capability under visible irradiation (Ruzimuradov et al. 2014). Previously (Ihara et al. 2003), oxygen vacancies are suggested to cause visible-light activity, hence the addition of
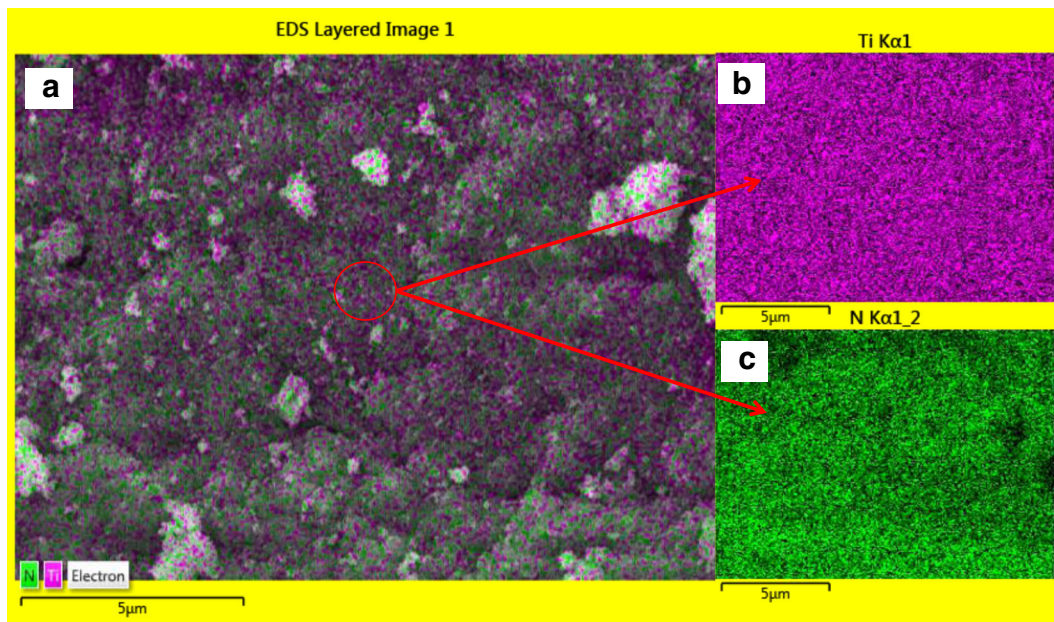

Fig. 6 EDX image of N-dopant present in the prepared TiO_2 sample **a** N-doped TiO_2 particle and **b** EDX-mapping of Ti and N in N-doped TiO_2
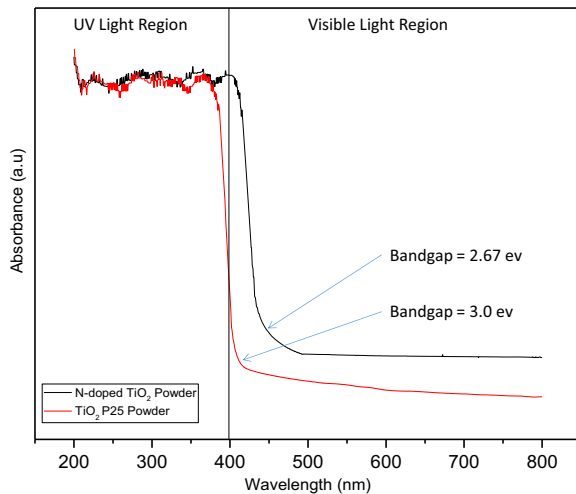
Fig. 7 UV–Vis absorption spectrum of N-doped TiO_2

nitrogen into TiO_2 lattice structure is believe to stabilize these oxygen vacancies to increase the sensitivity of the optical response to the visible-light region. The obtained band gap energy of the investigated N-doped TiO_2 is 2.67 eV, which is lower compared to commercial TiO_2 P25. This narrow band gap will strongly influence the photocatalytic action of the N-doped TiO_2 under visible-light irradiation. Interestingly, the prepared N-doped TiO_2 exhibited almost similar optical responses to UV region as compared to commercial TiO_2 P25; hence, it is believed that the prepared sample is able to develop photocatalytic property as comparably good as commercial TiO_2 P25 under UV-light irradiation (Fig. 7).

3.5 Photocatalytic Degradation of BPA and RB5

The photocatalytic degradation of BPA and RB5 in aqueous solution has been conducted to evaluate the photocatalytic efficiency of the prepared N-doped TiO_2 under visible- and UV-light irradiation in comparison with commercial TiO_2 P25. Figure 8 shows the adsorption activity of both contaminants without visible-light irradiation conducted for 60 min. It is indicated that the adsorption capacity of the prepared N-doped TiO_2 had reached equilibrium at 30 min for both BPA and RB5. Therefore, each experiment was irradiated using visible light/UV light after 30 min to standardize the experiment. Figure 9 demonstrates the evaluation of photocatalytic activity of N-doped TiO_2 particles under visible- and UV-light irradiation in comparison with commercial TiO_2 P25. As can be seen in Fig. 9, the prepared N-doped TiO_2 had photocatalytic activity under visible-light irradiation with 91.3% and 89.1% degradation of BPA and RB5 was achieved after 360 min, respectively. In addition, low reduction of 3.7% and 4.5% of BPA and RB5 concentration, respectively, was observed without visible-light irradiation, which shows that the system has reached the adsorption–desorption equilibrium. It is indicated that the photocatalytic degradation of the BPA can occur only with the present of photocatalyst and light irradiation. Meanwhile, TiO_2 P25 had very low photocatalytic activity under visible-light irradiation with degradation percentages of 11.3% and
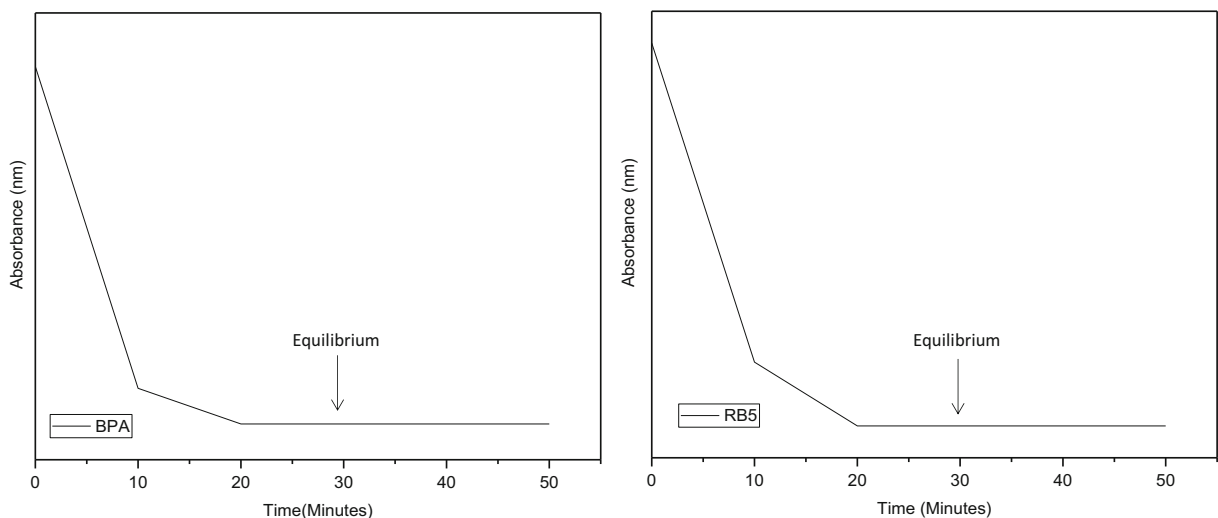

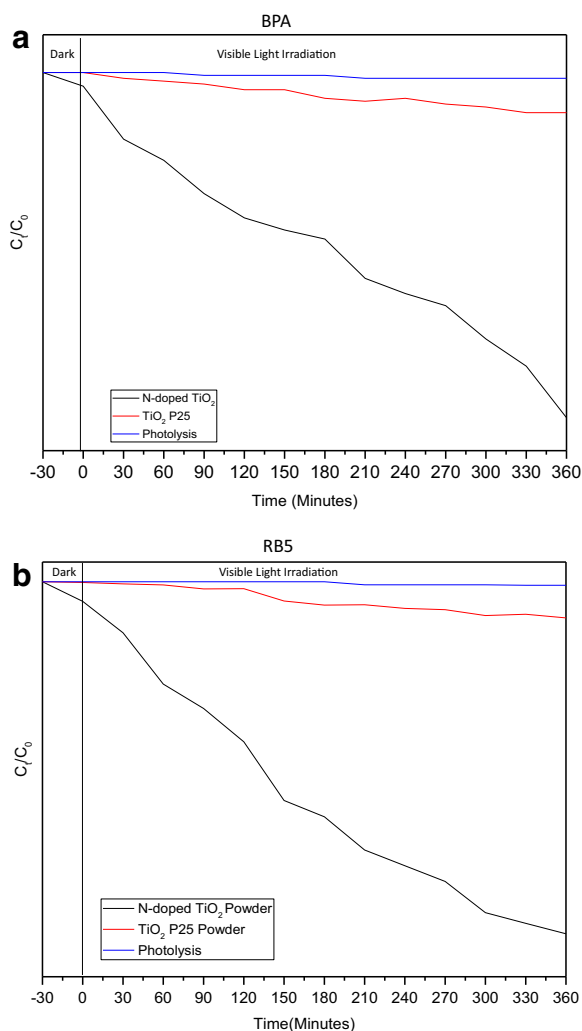**Fig. 8** Adsorption test of BPA and RB5 by N-doped TiO_2

Fig. 9 Photocatalytic degradation of **a** BPA and **b** RB5 by N-doped TiO_2 and TiO_2 P25 under visible-light irradiation

9.1% of BPA and RB5 after 360 min of activity, respectively. The efficient photocatalytic property of the prepared N-doped TiO_2 under visible-light irradiation is believed due to the present of nitrogen atom in TiO_2 lattice structure which enhances the absorption capability in visible-light irradiation. Hence, the efficiency of photocatalytic activity N-doped TiO_2 under visible-light irradiation suit for a broad range of photocatalytic application for the elimination of various water contaminants. Findings in this photocatalytic degradation of BPA by the prepared N-doped TiO_2 are in agreement with similar trend in degradation of methylene blue and phenol by previously reported studies (Mohamed et al. 2015a, b).

4 Conclusions

The N-doped TiO_2 were successfully synthesized by simple sol–gel method. The formation of anatase/rutile mixed phase TiO_2 microspheres is constituted by assembled TiO_2 nanorods as confirmed via FE-SEM and XRD analysis. The introduction of nitrogen doping in the TiO_2 lattice structure was observed by FTIR and EDX-mapping analysis. The results proved that the resultant N-doped TiO_2 exhibited good optical properties with excellent degradation properties up to 90% under visible-light irradiation. Therefore, in the future, the incorporation of N-doped TiO_2 nanoparticles in the hollow fiber membrane matrix would offer a great treatment for simultaneous separation and degradation of contaminants from water which leads to the complete safe and clean water sources to fulfill the public demands.

References

Abadias, G., Paumier, F., Eyidi, D., et al. (2010). Structure and properties of nitrogen-doped titanium dioxide thin films produced by reactive magnetron sputtering. *Surface and Interface Analysis, 42*, 970–973. https://doi.org/10.1002/sia.3220.

Ananpattarachai, J., Kajitvichyanukul, P., & Seraphin, S. (2009). Visible light absorption ability and photocatalytic oxidation activity of various interstitial N-doped TiO2 prepared from different nitrogen dopants. *Journal of Hazardous Materials, 168*, 253–261. https://doi.org/10.1016/j.jhazmat.2009.02.036.

Balakrishnan, M., Antony, A. S., Gunasekaran, S., & Natarajan, R. K. (2008). Impact of dyeing industrial effluents on the groundwater quality in Kancheepuram (India). *Indian Journal of Science and Technology, 1*, 1.

Chen, J., Cen, J., Xu, X., & Li, X. (2016). The application of heterogeneous visible light photocatalysts in organic synthesis. *Catalysis Science & Technology, 6*, 349–362. https://doi.org/10.1039/C5CY01289A.

Chong, M. N., Jin, B., Chow, C. W. K., & Saint, C. (2010). Recent developments in photocatalytic water treatment technology: a review. *Water Research, 44*, 2997–3027. https://doi.org/10.1016/j.watres.2010.02.039.

Dharma, J., & Pisal, A. (2009). *Simple method of measurement the band gap energy value of TiO₂ in the powder form using UV/*

Vis/NIR spectrometer, app note (pp. 1–4). Waltham: Perkin Elmer Inc..

Gai, L., Duan, X., Jiang, H., et al. (2012). One-pot synthesis of nitrogen-doped TiO2 nanorods with anatase/brookite structures and enhanced photocatalytic activity. *CrystEngComm, 14,* 7662. https://doi.org/10.1039/c2ce25563d.

Grasselli, F., Baratta, L., Baioni, L., et al. (2010). Bisphenol A disrupts granulosa cell function. *Domestic Animal Endocrinology, 39,* 34–39. https://doi.org/10.1016/j.domaniend.2010.01.004.

Hu, L., Wang, J., Zhang, J., et al. (2014). An N-doped anatase/rutile TiO $_2$ hybrid from low-temperature direct nitridization: enhanced photoactivity under UV-/visible-light. *RSC Advances, 4,* 420–427. https://doi.org/10.1039/C3RA44421J.

Ihara, T., Miyoshi, M., Iriyama, Y., et al. (2003). Visible-light-active titanium oxide photocatalyst realized by an oxygen-deficient structure and by nitrogen doping. *Applied Catalysis B: Environmental, 42,* 403–409. https://doi.org/10.1016/S0926-3373(02)00269-2.

Jańczyk, A., Krakowska, E., Stochel, G., & Macyk, W. (2006). Singlet oxygen photogeneration at surface modified titanium dioxide. *Journal of the American Chemical Society, 128,* 15574–15575. https://doi.org/10.1021/ja065970m.

Jinlong, L., Xinxin, M., Mingren, S., et al. (2010). Fabrication of nitrogen-doped mesoporous TiO2 layer with higher visible photocatalytic activity by plasma-based ion implantation. *Thin Solid Films, 519,* 101–105. https://doi.org/10.1016/j.tsf.2010.07.070.

Kafizas, A., Crick, C., & Parkin, I. P. (2010). The combinatorial atmospheric pressure chemical vapour deposition (cAPCVD) of a gradating substitutional/interstitial N-doped anatase TiO 2 thin-film; UVA and visible light photocatalytic activities. *Journal of Photochemistry and Photobiology A: Chemistry, 216,* 156–166. https://doi.org/10.1016/j.jphotochem.2010.06.034.

Lang, I. A. (2008). Association of urinary bisphenol A concentration with medical disorders and laboratory abnormalities in adults. *JAMA, 300,* 1303. https://doi.org/10.1001/jama.300.11.1303.

Lazim, Z. M., Zulkifli, N. S., Hadibarata, T., & Yusop, Z. (2015). Removal of cresol red and reactive black 5 dyes by using spent tea leaves and sugarcane baggase powder. *Jurnal Teknologi, 74*(11), 147–151.

Lee, J., Kim, J., & Choi, W. (2011). TiO 2 Photocatalysis for the redox conversion. *Aquatic Redox Chemistry, 10.* https://doi.org/10.1021/bk-2011-1071.ch010.

Lee, H. U., Lee, Y. C., Lee, S. C., et al. (2014). Visible-light-responsive bicrystalline (anatase/brookite) nanoporous nitrogen-doped TiO2photocatalysts by plasma treatment. *Chemical Engineering Journal, 254,* 268–275. https://doi.org/10.1016/j.cej.2014.06.011.

Lenie, S., Cortvrindt, R., Eichenlaub-Ritter, U., & Smitz, J. (2008). Continuous exposure to bisphenol a during in vitro follicular development induces meiotic abnormalities. *Mutation Research, Genetic Toxicology and Environmental Mutagenesis, 651,* 71–81. https://doi.org/10.1016/j.mrgentox.2007.10.017.

Li, X., Ying, G. G., Su, H. C., et al. (2010). Simultaneous determination and assessment of 4-nonylphenol, bisphenol a and triclosan in tap water, bottled water and baby bottles.

Environment International, 36, 557–562. https://doi.org/10.1016/j.envint.2010.04.009.

Liu, T., et al. (2015). Fabrication of a dual-layer (CA / PVDF) hollow fi ber membrane for RO concentrate treatment. *Desalination, 365,* 57–69. https://doi.org/10.1016/j.desal.2015.02.020.

Meeker, J. D., & Ferguson, K. K. (2011). Relationship between urinary phthalate and bisphenol a concentrations and serum thyroid measures in U.S. adults and adolescents from the National Health and nutrition examination survey (NHANES) 2007-2008. *Environmental Health Perspectives, 119,* 1396–1402. https://doi.org/10.1289/ehp.1103582.

Milić, N., Četojević-Simin, D., Milanović, M., et al. (2015). Estimation of in vivo and in vitro exposure to bisphenol A as food contaminant. *Food and Chemical Toxicology, 83,* 268–274. https://doi.org/10.1016/j.fct.2015.07.003.

Mohamed, M. A., Salleh, W. N. W., Jaafar, J., et al. (2015a). Photodegradation of phenol by N-doped TiO2 anatase/rutile nanorods assembled microsphere under UV and visible light irradiation. *Materials Chemistry and Physics, 162,* 113–123. https://doi.org/10.1016/j.matchemphys.2015.05.033.

Mohamed, M. A., Salleh, W. N. W., Jaafar, J., & Ismail, A. F. (2015b). Structural characterization of N-doped anatase–rutile mixed phase TiO2 nanorods assembled microspheres synthesized by simple sol–gel method. *Journal of Sol-Gel Science and Technology, 74,* 513–520. https://doi.org/10.1007/s10971-015-3627-2.

Moharram, A. H., Mansour, S. A., Hussein, M. A., & Rashad, M. (2014). Direct precipitation and characterization of ZnO nanoparticles. *Journal of Nanomaterials, 2014.* https://doi.org/10.1155/2014/716210.

Nakata, K., & Fujishima, A. (2012). TiO2 photocatalysis: design and applications. *Journal of Photochemistry and Photobiology C Photochemistry Reviews, 13,* 169–189. https://doi.org/10.1016/j.jphotochemrev.2012.06.001.

O'Shea, K. E., & Dionysiou, D. D. (2012). Advanced oxidation processes for water treatment. *Journal of Physical Chemistry Letters, 3,* 2112–2113.

Pelaez, M., Nolan, N., & Seery, M. (2012). A review on the visible light active titanium dioxide photocatalysts for environmental applications. *Applied Catalysis B: Environmental, 125,* 331–349. https://doi.org/10.1016/j.apcatb.2012.05.036.

Pore, V., Heikkilä, M., Ritala, M., et al. (2006). Atomic layer deposition of TiO2-xNx thin films for photocatalytic applications. *Journal of Photochemistry and Photobiology A: Chemistry, 177,* 68–75. https://doi.org/10.1016/j.jphotochem.2005.05.013.

Qiao, M., Chen, Q., Wu, S., & Shen, J. (2010). Novel sol-gel synthesis of N-doped TiO2 hollow spheres with high photocatalytic activity under visible light. *Journal of Sol-Gel Science and Technology, 55,* 377–384. https://doi.org/10.1007/s10971-010-2253-2.

Ruan, P., Qian, J., Xu, Y., et al. (2013). Mixed-phase TiO2 nanorods assembled microsphere: crystal phase control and photovoltaic application. *CrystEngComm, 15,* 5093. https://doi.org/10.1039/c3ce40351c.

Ruzimuradov, O., Nurmanov, S., Hojamberdiev, M., et al. (2014). Fabrication of nitrogen-doped TiO2 monolith with well-defined macroporous and bicrystalline framework and its photocatalytic performance under visible light. *Journal of*

the *European Ceramic Society, 34*, 809–816. https://doi.org/10.1016/j.jeurceramsoc.2013.10.009.

Shah, M. P., & Patel, K. A. (2014). Microbial degradation of reactive red 195 by three bacterial isolates in anaerobic-aerobic bioprocess. *International Journal of Environmental Bioremediation & Biodegradation, 2*, 5–11.

Takai, Y., Tsutsumi, O., Ikezuki, Y., et al. (2000). Estrogen receptor-mediated effects of a xenoestrogen, bisphenol A, on preimplantation mouse embryos. *Biochemical and Biophysical Research Communications, 270*, 918–921. https://doi.org/10.1006/bbrc.2000.2548.

Takeuchi, T., Tsutsumi, O., Ikezuki, Y., et al. (2004). Positive relationship between androgen and the endocrine disruptor, bisphenol A, in normal women and women with ovarian dysfunction. *Endocrine Journal, 51*, 165–169. https://doi.org/10.1507/endocrj.51.165.

Tang, W. Z., & An, H. (1995). UV/TiO$_2$ photocatalytic oxidation of commercial dyes in aqueous solutions. *Chemosphere, 31*(9), 4157–4170.

Ugurlu, M., Gürses, A., & Dogar, C. (2007). Adsorption studies on the treatment of textile dyeing effluent by activated carbon prepared from olive stone by ZnCl2 activation. *Coloration Technology, 123*(2), 106–114.

Umar, M., & Abdul Aziz, H. (2013). Photocatalytic degradation of organic pollutants in water. Organic pollutants - monitoring, risk and treatment. In Nageeb Rashed, M. (Ed.), ISBN: 978-953-51-0948-8, InTech. https://doi.org/10.5772/53699. Available from: http://www.intechopen.com/books/organic-pollutants-monitoring-risk-and-treatment/photocatalytic-degradation-of-organic-pollutants-in-water.

Vandenberg, L. N., Hauser, R., Marcus, M., et al. (2007). Human exposure to bisphenol A (BPA). *Reproductive Toxicology, 24*, 139–177. https://doi.org/10.1016/j.reprotox.2007.07.010.

Viswanathan, B., & Krishanmurthy, K. R. (2012). Nitrogen incorporation in TiO$_2$: does it make a visible light photo-active material? *International Journal of Photoenergy, 2012*. https://doi.org/10.1155/2012/269654.

Wang, R., Hashimoto, K., Fujishima, A., Chikuni, M., Kojima, E., Kitamura, A., Shimohigoshi, M., & Watanabe, T. (1997). Light-induced amphiphilic surfaces. *Nature, 388*, 431–432.

Zainudin, N. S., Yaacoba, M. H., & Othman, Z. (2016). Stability of reactive black 5 (RB5) standard solution studied in different conditions. *Health and the Environment Journal, 7*(1), 87–100.

Zhang, Y. C., Yang, M., Zhang, G., & Dionysiou, D. D. (2013). HNO3-involved one-step low temperature solvothermal synthesis of N-doped TiO2 nanocrystals for efficient photocatalytic reduction of Cr(VI) in water. *Applied Catalysis B: Environmental, 142–143*, 249–258. https://doi.org/10.1016/j.apcatb.2013.05.023.

Zhao, L., Jiang, Q., & Lian, J. (2008). Visible-light photocatalytic activity of nitrogen-doped TiO2 thin film prepared by pulsed laser deposition. *Applied Surface Science, 254*, 4620–4625. https://doi.org/10.1016/j.apsusc.2008.01.069.